

Particle-like light structures in a wide-aperture laser with saturable absorption

N. N. Rozanov, A. V. Fëdorov, S. V. Fëdorov, and G. V. Khodova

Laser Physics Scientific-Research Institute associated with the S.I. Vavilov State Optical Institute, 199034 St. Petersburg, Russia

(Submitted 29 July 1994)

Zh. Eksp. Teor. Fiz. **107**, 376–392 (February 1995)

An analysis is given of laser autosolitons—localized light structures—and of the interactions of pairs of such autosolitons in a wide-aperture laser with saturable absorption. Stationary and propagating autosolitons with wavefront dislocations (vortices) have been found. Reflection of autosolitons from the mirrors of the laser cavity is studied. Two colliding laser autosolitons display the regime of weak interactions (in which autosoliton characteristics vary little after the collision) and the regime of strong interactions (where the number of autosolitons changes). © 1995 American Institute of Physics.

1. INTRODUCTION

The formation of spatial and temporal field structures due to spontaneous symmetry violation in nonlinear-optical systems which are homogeneous in space and time takes place according to two different scenarios. The first is connected with the loss of stability of the homogeneous field distribution, which leads to filamentation: a) to small-scale self-focusing and breakup of the beam in the transverse direction (relative to the main direction of propagation) into separate, intense filaments, and b) to modulational instability and breakup of a long pulse into separate short pulses. Related studies, initiated by the work of Bespalov and Talanov,¹ have had great practical importance since small-scale self-focusing is the main obstacle to increasing the intensity of high-power pulsed lasers. As a result, various approaches to suppressing such instabilities have been proposed.² In addition, filamentation conditions lead to the appearance of localized (particle-like or soliton-like) light structures. The simultaneous development of instabilities in the transverse and longitudinal directions has given rise to the important concept of three-dimensional solitons, or “light bullets.”³ If in systems without feedback these instabilities are convective (the perturbations grow with increase of the longitudinal coordinate), then in the presence of feedback, e.g., in a nonlinear interferometer, the instabilities are absolute (they increase in time at a given position).⁴

The second scenario does not require loss of instability of spatially homogeneous regimes. In this case, soliton-like structures are rigidly excited by a large initial perturbation, whereas weak perturbations against a background of a stable, spatially homogeneous distribution disperse. Such localized structures are known for a wide class of open, nonlinear systems of varying physical nature, and in the Russian literature they are frequently called autosolitons.⁵ The characteristics of these autosolitons do not depend on the details of the initial perturbation, so these structures are quite rigid. What is important is that in optics there now is a new mechanism of spatial coupling of the elements of an optical system, namely a diffraction mechanism, alongside the previously considered diffusion mechanism.⁵ This factor is responsible for a number of the properties of “diffraction autosolitons,” both theoretical^{6,7} and experimental⁸ in wide-aperture non-

linear interferometers [see Ref. 9 (review)]. Note that diffusion autosolitons also exist in passive nonlinear interferometers with competing nonlinearities.¹⁰

“Laser autosolitons” (a related type of autosoliton) have been theoretically predicted in wide-aperture lasers with an additional nonlinear element possessing saturable absorption.^{11,12} As is well known,¹³ rigid excitation of lasing is achieved in such lasers and the dependence of the lasing power on the gain coefficient has a hysteretic character. Laser autosolitons are stationary islands of lasing, which is absent from the rest of the laser aperture. They can move in the transverse direction with arbitrary speed (but much less than the speed of light). In this regard, a mechanical model can be constructed of a single laser autosoliton in a laser with smoothly varying parameters, e.g., in the case of curved mirrors at the ends of the cavity.¹⁴ When the lasing threshold is only slightly exceeded, the existence of transversely one-dimensional laser autosolitons follows from the results of Ref. 15.

Comparison of localized clots of light to particles, disregarding their internal structure, has, naturally, a limited domain of applicability. This is manifested with especial clarity in the interactions of such “particles”. If this interaction is weak (only the peripheral regions of the soliton-like excitations, where the intensity is low, overlap), then changes in the characteristics of the “particles” occasioned by the interaction are small and can be delineated within the framework of perturbation theory.¹⁶ In strong interactions, on the other hand, when even the number of “particles” can change as a result of the collision, analysis is hindered and almost inevitably reduces (at least initially) to numerical modeling. Note that a knowledge of the elementary laws of the interaction of the two laser autosolitons is necessary in the subsequent construction of the theory of the autosoliton “gas” and the formation of autosoliton lattices, analyzing the optical turbulence regimes, etc.

In the present article, we use numerical modeling to do the first-ever study of collisions of two laser autosolitons in both the weak- and strong-interaction regimes. In Sec. 2 we write out the basic equations and discuss the properties of isolated laser autosolitons. In particular, we demonstrate here for the first time the existence of stable laser autosolitons

with wavefront dislocations (vortices). Further calculations are carried out in the geometry with transverse dimension. This shortens the calculation time and is justified for a laser scheme in the form of a planar waveguide in one of the transverse directions. Besides, these equations and their solutions are of independent interest. Specifically, by means of a space-time analogy, they describe the propagation of pulses in a single-mode nonlinear waveguide which includes elements with saturable gain and absorption.¹⁷ In Sec. 3 we study the previously discussed problem of reflection of laser autosolitons from the edge of the mirror of the laser cavity. Here it is important for us to show that because of such reflections the autosoliton is preserved in a finite-aperture laser for an unlimited time. The first results of our analysis of the collision of two initially far-apart laser autosolitons are presented in Sec. 4. The main results are summarized in the Conclusion.

Note that laser solitons differ substantially in their properties both from diffraction autosolitons in passive nonlinear interferometers, excited by external radiation, and from diffusion autosolitons. A detailed comparison of these three types of structures is given in Ref. 14. Here we remark that we do not know of any analogs from the diffusion autosoliton region to the laser autosolitons with wavefront dislocations obtained in the present work: in fact, it is questionable whether the very concept of a wavefront is appropriate for the “incoherent” systems considered, for example, in Ref. 5. If the velocity of a diffusion autosoliton is completely determined by the parameters of the system and is established independently of the initial conditions, then for a laser autosoliton the speed of transverse motion is arbitrary and is determined by the initial conditions. This difference arises because a light ray in a laser can have an arbitrary direction (within certain limits) relative to the cavity axis, a situation that is not observed for the usual transport processes described by the diffusion equations. Also, the physics of the interaction of diffusion autosolitons differs substantially from that of laser solitons. For example, laser autosolitons colliding with large relative velocity “rush through” each other so fast that their characteristics after the collision differ only slightly from before. Such a situation is excluded for diffusion autosolitons for quite obvious reasons. Still more different is the physics of the interaction between laser autosolitons with two transverse dimensions and wavefront dislocations, which will be the subject of later work.

2. BASIC EQUATIONS AND PROPERTIES OF ISOLATED LASER AUTOSOLITONS

We will take as our point of departure the equation proposed by Suchkov¹⁸ for the slowly varying field amplitude E in a wide-aperture laser:

$$2i \frac{k}{c} \frac{\partial E}{\partial t} + \Delta_{\perp} E + 4\pi \left(\frac{\omega}{c} \right)^2 \delta P + i \frac{2k}{L} (1-R)E = 0. \quad (2.1)$$

Here k , c , and ω are the wave number, speed of light, and frequency, t is the time, Δ_{\perp} is the transverse Laplacian, δP is the nonlinear component of the polarization of the medium, which is assumed to be homogeneous and isotropic, L is the

length of the cavity, and R is the product of the amplitude reflection coefficients of its mirrors. This equation can be obtained by averaging the quasi-optical equation in the longitudinal direction z under the assumption that the field varies little during the time τ required for the radiation to pass through the cavity. This equation correctly describes the transverse structure of the field not only in the regime of a single longitudinal mode, but also for a sufficiently narrow lasing spectrum (see Refs. 11 and 12):

$$\delta\lambda/\lambda \ll N_F^{-1/2}. \quad (2.2)$$

Here $\delta\lambda/\lambda$ is the relative width of the lasing spectrum, and N_F is the Fresnel number of the cavity. Under real conditions, inequality (2.2) is satisfied even for wide-aperture lasers by virtue of the extraordinary narrowness of the lasing spectrum.

Within the scope of Eq. (2.1) it is possible also to analyze manifestations of smooth transverse and temporal variation of the medium and cavity. For example, the transverse variation of the reflection coefficient of the mirrors is taken into account by the function $R(\mathbf{r})$, where \mathbf{r} is the two-component vector of the transverse coordinates. Generalization of this equation with inclusion of external radiation¹⁹ describes transverse effects in a nonlinear interferometer (including switching waves and diffraction autosolitons⁹).

Let us specify the form of the polarization of the nonlinear medium. We will assume that two kinds of two-level atoms are present inside the laser: respectively, atoms with (continuous pumping) and without population inversion. For monochromatic radiation and coincidence of the frequencies of the field and the atomic transitions, we have in the steady-state regime

$$\delta P = -i\varepsilon_0 \left(\frac{\alpha_0}{1+I/I_{\alpha}} - \frac{\beta_0}{1+I/I_{\beta}} \right) \frac{E}{4\pi k}, \quad (2.3)$$

where ε_0 is the nonresonance (linear) part of the dielectric constant of the medium, α_0 and β_0 are the coefficients of saturable gain and absorption, I_{α} and I_{β} are the intensities of saturation of the active and passive components of the medium, and $I = |E|^2$ is the local intensity.

We will neglect transition processes in the medium, assuming that the relaxation times of the medium are considerably less than the characteristic time scales of variation of the field (class-A laser; finite relaxation times do not noticeably influence the properties of sufficiently slow-moving laser autosolitons²⁰). Then Eqs. (2.1) and (2.3) give a closed description of transverse effects in the laser.

Before discussing various laser regimes, let us note some general properties of the solutions of Eqs. (2.1) for which the noninertial nonlinearities of the medium have arbitrary form $\delta P = \chi(|E|^2)E$. Say we know some solution $E_0(\mathbf{r}, t)$ of Eq. (2.1), then the following functional forms can serve as solutions of this equation:

$$E(\mathbf{r}, t) = E_0(\mathbf{r} - \mathbf{r}_0, t - t_0), \quad (2.4)$$

$$E(\mathbf{r}, t) = E_0(\mathbf{r}, t) \exp(i\Phi), \quad (2.5)$$

$$E(\mathbf{r}, t) = E_0(\mathbf{r} - \mathbf{v}t, t) \exp\left(i \frac{k}{c} \mathbf{v} \mathbf{r}\right) \exp\left(-i \frac{k}{2c} \mathbf{v}^2 t\right). \quad (2.6)$$

Here we have introduced arbitrary scalar (t_0 and Φ) and two-component vector (\mathbf{r}_0 and \mathbf{v}) constants. Relation (2.4) corresponds to a homogeneous system in space (in the transverse coordinates) and time, where \mathbf{r}_0 and t_0 correspond to an arbitrary shift in the transverse coordinates and time. Relation (2.5) displays the arbitrariness of the total phase of the field. Finally, relation (2.6) corresponds to arbitrariness in the choice of the direction of the preferred direction of propagation and puts each solution in correspondence with a family of other solutions for which the velocity of transverse motion of the field envelope is shifted by \mathbf{v} , with an additional wavefront wedge (proportional to \mathbf{v}) and frequency shift proportional to v^2 .

The simplest (trivial) regimes that can be described by Eq. (2.1) are the nonlasing regime and the plane-wave regimes. The nonlasing regime ($E_0=0$) is stable if

$$C_\alpha - C_\beta < 1, \quad (2.7)$$

where $C_\alpha = \alpha_0 L / 2(1 - R)$, $C_\beta = \beta_0 L / 2(1 - R)$. We can write this condition in the form $g_0 < g_{\max}$ (where $g_0 = \alpha_0 L$ is the gain, and we assume it to be fulfilled).

The plane-wave regimes correspond to a field of the form

$$E = A \exp(i\mathbf{q}\mathbf{r}) \exp[i(\nu t + \Phi)]. \quad (2.8)$$

Here Φ is an arbitrary phase, \mathbf{q} is the transverse component of the wave vector, $\nu = -c\mathbf{q}^2/2k$ is the frequency shift, and the amplitude A can be assumed to be real and related to the intensity of the wave I by the formula $I = A^2$. The intensity is determined by the quadratic equation

$$I^2 - [I_\alpha(C_\alpha - 1) - I_\beta(C_\beta + 1)]I + (1 - C_\alpha + C_\beta)I_\alpha I_\beta = 0. \quad (2.9)$$

It is not hard to determine the conditions under which this equation has two (positive) stationary solutions I_s and I_u . The smaller value (I_u) corresponds to unstable regimes. Then we have bistability: for the same gain $g_0 = \alpha_0 L$ in the interval

$$g_{\min} < g_0 < g_{\max} \quad (2.10)$$

either the nonlasing regime (intensity $I_0=0$) or the plane-wave regime with intensity I_s can be realized (Fig. 1). According to Eq. (2.8), these plane waves are characterized by different (arbitrary, but small) values of the angle between the propagation direction of the wave and the axis and corresponding (quadratic in the angle) frequency shifts. In this way we have a continuous spectrum of plane waves with the same value of the intensity. This situation can be compared with the continuous spectrum of transverse modes in an infinite-aperture laser. In a real laser, with a finite aperture, the plane-wave regimes are significantly altered; what happens here with the nontrivial (transversely inhomogeneous) regimes—the regimes that will be of interest to us in what follows—we will elucidate in the following section.

The fundamental regimes with transverse variation include switching waves and laser autosolitons. Switching waves exist inside every bistability interval (2.10) and are

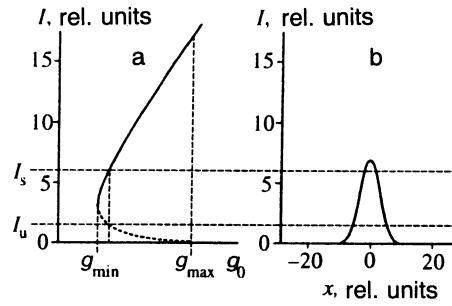


FIG. 1. a) Dependence of the lasing intensity on the gain in the plane-wave regime. Dashed line corresponds to unstable regimes; b) intensity profile of a laser autosoliton: $g_0=2.06$, $R=0.9$, $\beta_0 L=2.0$, $I_\alpha=10I_\beta$.

fronts of switching between two stable trivial states (with intensities $I_0=0$ and I_s), translating in the transverse direction with constant velocity \mathbf{v} . The field intensity approaches these values at sufficient distances from the wavefront, on either side. Switching waves exist in a wide-aperture laser for both the diffusion²¹ and the diffraction^{11,12} mechanisms of transverse coupling. The “Maxwell value” g_M (or some other control parameter), which is defined in the following manner, plays an important role here. If lasing with intensity $\sim I_s$ is initially present over a finite (large in comparison with the width of the switching wavefront) region of the laser aperture, then as a result of the motion of the switching wavefronts the lasing region will narrow in time for $g_0 < g_M$ and increase for $g_0 > g_M$.

Laser autosolitons exist in some gain interval narrower than the bistability interval (2.10) and including the “Maxwell value” of the gain g_M .^{11,12} The simplest (immobile or stationary) laser autosoliton is characterized by a field distribution of the form

$$E = G(\mathbf{r}) \exp(i\nu^{(0)}t). \quad (2.11)$$

Here $\nu^{(0)}$ is the lasing frequency shift, defined by the laser parameters, and is due to the combined action of the diffraction and nonlinear effects. The intensity profile $I = |G(\mathbf{r})|^2$ (Fig. 1b) possesses a characteristic width $w_0 \sim 4w = 4\sqrt{\lambda L/4\pi(1-R)}$, where w is the width of the switching wave. Note that along with the simple bell-shaped profile, laser autosolitons can possess a more complicated field distribution, including screw dislocations of the wavefront. In this case, in the geometry with two transverse dimensions, using polar coordinates we can write

$$G(\mathbf{r}) = G_m(r) \exp(im\varphi), \quad m = 0, \pm 1, \pm 2, \dots \quad (2.12)$$

The azimuthal number (topological charge) m determines the rate of falloff of the field at the dislocation center ($G_m(r) \sim r^{|m|}$ as $r \rightarrow 0$) and the phase shift incurred upon one circulation around the center along a closed contour ($2\pi m$). Axially-symmetric laser autosolitons ($m=0$) with two transverse dimensions were demonstrated in Ref. 20. Our calculations demonstrate the existence of laser autosolitons with screw dislocations of first ($m=1$ or -1) and second ($m=2$ or -2) order. The initial field distribution is given in the form

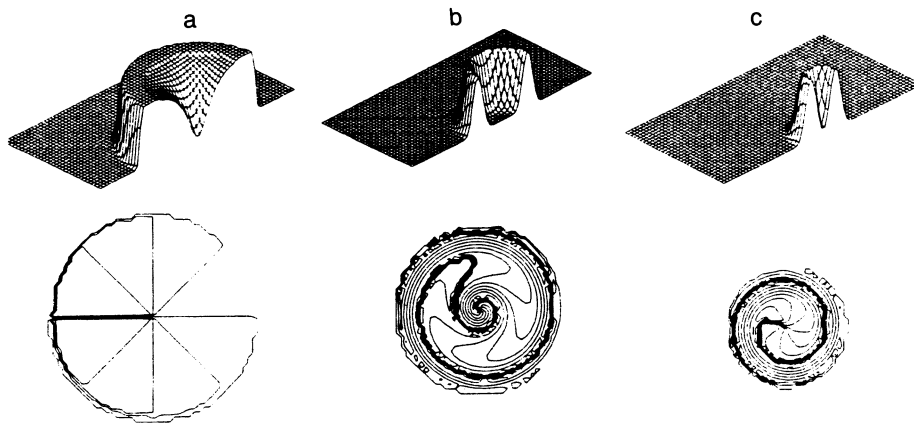


FIG. 2. Intensity profiles (upper figures) and phase isolines (with interval $\pi/4$, lower figures) in the formation of a laser autosoliton with a first-order wavefront dislocation ($m = 1$, $\delta r = 10w$, $r_0 = 30w$, $\delta r_0 = 0.1w$); a) $t = 0$, b) $t = 400$, c) $t = 1000$ (time in number of passes of the cavity).

$$G(\mathbf{r}) = \begin{cases} \sqrt{I_2} \{1 - \exp[-(r/\delta r)^{|m|}]\} \exp(im\varphi), & r < r_0, \\ \sqrt{I_2} \exp\{-[(r-r_0)/\delta r_0]^4\}, & r > r_0. \end{cases} \quad (2.13)$$

Here r_0 is the radial coordinate at which the intensity is maximum, and δr and δr_0 characterize the width of this maximum in the regions of smaller and larger r . Figure 2 depicts the formation of a laser autosoliton with a first-order dislocation. Time in this figure and in the figures that follow is in units of the time it takes light to make one pass across the cavity, τ . The intensity profiles are axially symmetric; initially two radial switching waves are formed in them at distances of roughly δr and $r_0 + \delta r_0$ from the center. Further motion of the switching waves in opposing directions leads to the formation of a ring-shaped laser autosoliton, whose radius $r(t)$ decreases with time (Fig. 2b). The local radial profiles of the intensity and phase do not change as long as $r(t) \geq 2w$. The mean value of the phase grows constantly in time, which is equivalent to the turning of the isolines like the hour-hand of a clock, or to a positive phase shift ν . Finally, after ~ 1000 passes, a field distribution is formed in the center of the established laser autosoliton (Fig. 2c) that is characteristic of a dislocation of the given order. Here the frequency shift of the dislocation laser autosoliton is, as before, nonzero, i.e., the established phase vortex, like the hour-hand of a clock, continues to turn. The kinetics of the establishment of a second-order dislocation laser autosoliton ($m=2$) is analogous. The laser autosolitons shown in Fig. 2 are stationary (in the transverse direction). At the same time, relation (2.6) means that dislocation laser autosolitons with field profile

$$E = G(\mathbf{r} - \mathbf{v}t) \exp[i(k/c)\mathbf{v}\mathbf{r}] \exp(i\nu t). \quad (2.14)$$

moving with arbitrary (constant) velocity \mathbf{v} ($v/c \ll 1$) have been constructed. Here the frequency shift depends quadratically on the velocity:

$$\nu = \nu^{(0)} - (k/2c)\mathbf{v}^2. \quad (2.15)$$

3. INFLUENCE OF THE EDGES OF THE MIRRORS

When we take the edges of the mirrors into account, the plane-wave solutions discussed above lose their meaning. Empty-cavity modes correspond not to traveling waves (in the transverse direction), but to standing waves formed by

diffraction of the waves by the edges of the mirrors.^{22,23} Nonlinearity leads to distortions and interaction of modes. Regarding what is of interest to us here, laser autosolitons, it is important that because of the falloff of the field at the periphery of the autosoliton, the edge of the mirror does not affect the properties of the laser autosoliton as long as the distance from the center of the autosoliton to the nearest point on the edge of the mirror significantly exceeds the width of the autosoliton. Therefore the edges of the mirrors in a wide-aperture laser need to be included only for traveling autosolitons ($\mathbf{v} \neq 0$) during those time intervals when they approach one of the edges of the mirror. We will consider this problem in the present section.

An established laser soliton is characterized by the tilt angle of its direction of propagation with the cavity axis $\theta = v/c$ and the width of the angular (diffractive) divergence $\theta_d \sim \lambda/w_0$, where λ is the wavelength of the light and w_0 is the characteristic width of the autosoliton. Of course, at large angles $\theta > \theta_c$ a laser soliton heading for the edge of the mirror will escape from the cavity and disappear, at which point lasing will cease. At the same time, at small angles the magnitude of the coefficient of diffractive reflection of plane waves approaches unity.²² We should therefore expect that for $\theta < \theta_c$ the laser autosoliton will be reflected from the edge of the mirror and move away from it. It is natural to assume that the critical angle θ_c at which the geometric transport of the autosoliton and diffractive spreading become comparable is equal to $\sim \theta_d$.

Our calculations confirm this qualitative picture. For simplicity here and below we consider a transversely one-dimensional laser scheme with the single transverse coordinate x . Although the reflection coefficient $R(x)$ of the mirrors varies abruptly at their edges, the approximation of the averaged quasi-optical equation (2.1) remains valid at small angles of incidence of the laser soliton ($\theta^2 \ll 1$), since then the field distribution changes little in one pass through the cavity. In this case an autosoliton should reflect from an edge of a mirror or escape from the cavity in this approximation during a time significantly exceeding the time of one traversal of the cavity, τ .

Results of our calculations are shown in Figs. 3–6. Figures 3 and 4 show the dynamics of the transverse profiles of

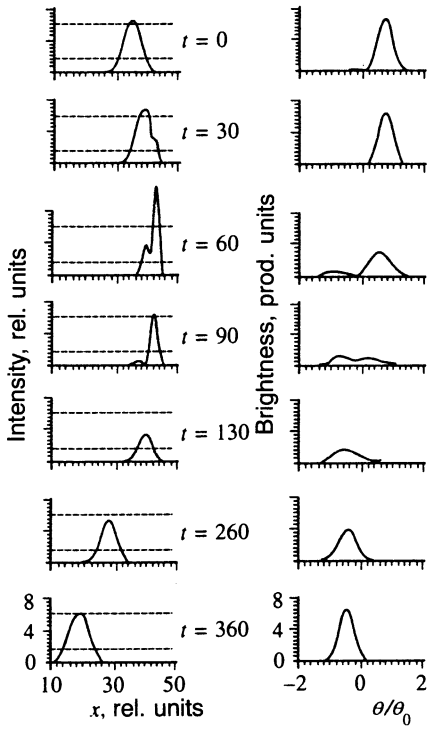


FIG. 3. Intensity profiles (left) and radiance distribution (right) for reflection of an autosoliton from the edge of the mirror at subcritical incidence angle $\theta=0.14\theta_0$.

the intensity (normalized to the saturation intensity I_β) and radiance (in arbitrary units)

$$J = \left| \int E(x,t) \exp(iqx) dx \right|^2 \quad (3.1)$$

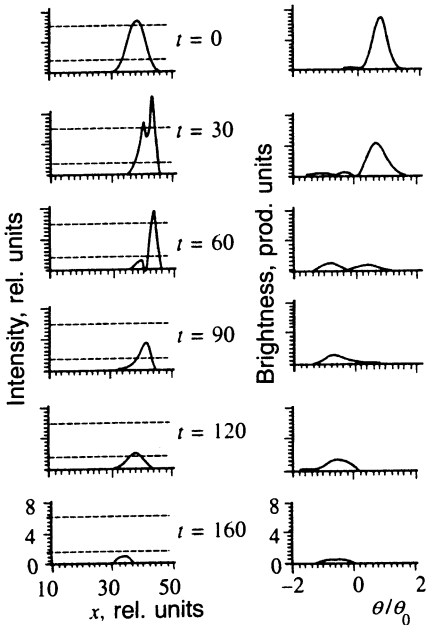


FIG. 4. The same as in Fig. 3, but for supercritical incidence angle $\theta=0.16\theta_0$.

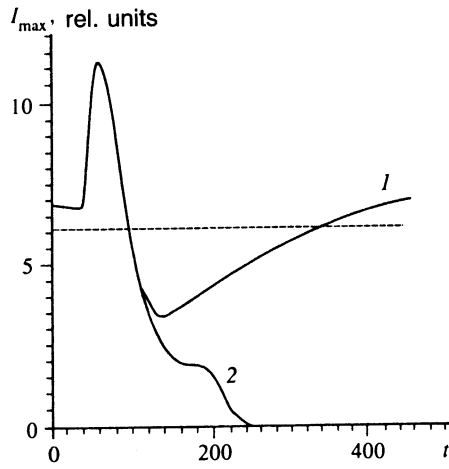


FIG. 5. Time dependence of the maximum intensity for reflection of an autosoliton with incidence angle $\theta=0.14\theta_0$ (1) and $\theta=0.16\theta_0$ (2).

(as a function of the angle $\theta=q/k$, in units of $\theta_0 = \sqrt{\lambda/L}$) for subcritical and supercritical incidence angles. Figures 5 and 6 show the time dependence of the maximum intensity I_{\max} and the coordinate of this maximum, x_{\max} , for laser parameters $R=0.9$, $\alpha_0 L=2.06$, $\beta_0 L=2.0$, and saturation intensity $I_\alpha=10I_\beta$. The intensity I is given in units of I_β , and its angular distribution (the radiance) is normalized to its maximum value J_{\max} . The x coordinate is expressed in units of w , the characteristic width of the switching wavefront (see above), and the edge of the mirror is at $x=45$.

For a subcritical angle of incidence (Fig. 3, $\theta=0.14\theta_0$), when the laser autosoliton reaches of the edge of the mirror ($t=30$) its intensity profile becomes deformed, to the extent that a second maximum forms near the boundary. In this case the radiance diagram acquires a second peak in the region of negative angles. Power gradually shifts into this peak out of the positive peak. Since the angle of incidence is near-critical, a significant amount of power is lost upon reflection ($t=130$), but the remaining part is large enough (it is super-

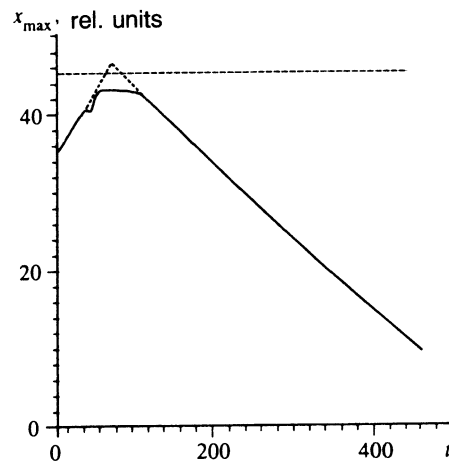


FIG. 6. Time dependence of the location of the maximum intensity of an autosoliton for reflection with incidence angle $\theta=0.14\theta_0$.

critical) that with time the laser autosoliton regains its stationary parameters ($t=360$). For a supercritical angle of incidence (Fig. 4, $\theta=0.16\theta_0$) the initial stage of the reflection is the same. However, the reflected part has subcritical power, and in time it dissipates (see also Fig. 5). In Fig. 6 one can make out some time delay upon reflection of the autosoliton, which is the temporal analog of a longitudinal shift of a beam when it reflects from the interface of linear media. In the same figure one can notice a decrease (of up to 30%) in the velocity of the reflection autosoliton in comparison with its velocity before reflection. This is due to the change in the radiance diagram brought about by the reflection (compare Fig. 3, $t=0$ and $t=360$), the maximum of which after reflection shifts toward smaller angles.

4. INTERACTION OF LASER AUTOSOLITONS

Let some spatially distributed laser autosolitons be excited in a laser (the distance between neighboring solitons δr_n significantly exceeds the width of an individual soliton, w_0). Then until the traveling autosolitons have begun to interact intensely, their field can be represented in the form [compare Eq. (2.14)]

$$E = \sum_n G(\mathbf{r} - \mathbf{r}_n - \mathbf{v}_n t) \exp\left(i \frac{k}{c} \mathbf{v}_n \mathbf{r}\right) \exp[i(\nu_n t + \Phi_n)]. \quad (4.1)$$

The constants \mathbf{r}_n , \mathbf{v}_n , ν_n , and Φ_n have their previous meaning. According to Eq. (4.1), to determine the field it is necessary to assign the initial localization (coordinates of the centers) of the individual autosolitons \mathbf{r}_n , and their velocities \mathbf{v}_n and phases Φ_n . The frequency shifts ν_n according to Eq. (2.15) are expressed in terms of the velocities \mathbf{v}_n .

$$\nu_n = \nu^{(0)} - (k/2c) \mathbf{v}_n^2. \quad (4.2)$$

Besides the "coordinate representation" (4.1), the angular spectrum of the field (its Fourier transformation with respect to the transverse coordinates) at some fixed moment of time t gives useful information. For an isolated, stationary ($\mathbf{v}_0=0$) laser autosoliton, localized at the origin ($\mathbf{r}_0=0$), the angular spectrum has the form

$$F_0(\mathbf{q}, t) = \exp(i\nu^{(0)} t) g(\mathbf{q}), \quad (4.3)$$

where

$$g(\mathbf{q}) = \int G(\mathbf{r}) \exp(i\mathbf{q}\mathbf{r}) d\mathbf{r}. \quad (4.4)$$

Note that the angular spectrum of one laser autosoliton $J_0(\mathbf{q}) = |F_0(\mathbf{q}, t)|^2 = |g(\mathbf{q})|^2$ does not depend on time. The width of its angular spectrum is proportional to w_0^{-1} .

The angular spectrum of a superposition of fields of several laser autosolitons is given by

$$F(\mathbf{q}, t) = \int E(\mathbf{r}, t) \exp(i\mathbf{q}\mathbf{r}) d\mathbf{r} = \sum_n g\left(\frac{k}{c} \mathbf{v}_n + \mathbf{q}\right) \times \exp\left[i\left(\frac{k}{c} \mathbf{v}_n \mathbf{r}_n + \mathbf{q}\mathbf{r}_n\right)\right] \exp[i(\nu_n t + \Phi_n)]. \quad (4.5)$$

Now the intensity of the angular spectrum varies with time quasiperiodically, and at a fixed time describes the interference (superposition taking phase into account) of the spectra of all of the autosolitons. When the velocities of the autosolitons differ significantly, i.e., when $\min|\delta\mathbf{v}| \gg c/kw_0$, the angular spectrum of the total field separates into the nonoverlapping (and noninterfering) spectra of the individual solitons. In the opposite limit $\max|\delta\mathbf{v}| \ll c/kw_0$, for small \mathbf{q} Eq. (4.5) can be replaced by the following approximate relation:

$$F(\mathbf{q}, t) = \sum_n \left\{ g \frac{k}{c} \mathbf{v}_n \exp[i(\nu_n t + \Phi_n)] \right\} \exp(i\mathbf{q}\mathbf{r}_n). \quad (4.6)$$

Here the spectral intensity as a function of \mathbf{q} includes oscillations with characteristic "angular frequencies" $\delta q_n \sim 2\pi/\delta r_n$. In other words, the further apart the various laser autosolitons are, the faster the amplitude of their radiance field oscillates. As the autosolitons get closer together, these oscillations increase in amplitude.

Let us now state the criterion for weak interaction of the laser autosolitons, which allows us to represent the field in the form (4.1). Usually, this criterion is formulated as a requirement that the spatial overlap of the fields of neighboring solitons be small, i.e., it is required that the field of each soliton be weak in the localization region of the other solitons. If this is the case, use of perturbation theory allows us to trace out small variations in the characteristics of the solitons as a result of their weak interaction.^{16,24} However, the interaction remains weak even when the laser autosoliton fields overlap completely if this overlap is short-lived, i.e., when the relative velocity (difference of velocities) $\delta\mathbf{v}$ of the solitons is large:²⁵

$$\min \delta\mathbf{v} \gg c(\omega_0/\lambda) |\delta\epsilon| \quad (4.7)$$

($\delta\epsilon$ is the nonlinear component of the dielectric constant). Here we have again justified the use of perturbation theory in the form proposed in Refs. 16 and 24. We will not give here the corresponding constructions, in light of their limited domain of applicability. Below we present results of a numerical analysis of strong as well as weak interaction of two initially separated laser autosolitons. For simplicity, we analyze only the case of a geometry with one transverse dimension. In the calculations we have used the same laser parameters as in Sec. 3; however, the radiance is given in the same (arbitrary) units. The two horizontal dashed lines in the graphs of the intensity profiles indicate the values I_s and I_u .

Consider first the symmetric collision of two laser autosolitons: $\mathbf{v}_2 = -\mathbf{v}_1$, $\Phi_2 = \Phi_1$. In this case the velocity of approach of the two solitons $\delta\mathbf{v} = 2\mathbf{v}_1$ and the phase difference remains zero. Figures 7–11 show how the dynamics of the collision changes as the relative velocity of the laser autosolitons decreases.

At large approach velocity (correspondingly, at large enough angles of incidence of the solitons), when condition (4.7) is satisfied, the autosolitons pass right through each other without any noticeable distortions of their shape or noticeable changes in their velocities and phases. The spatial intensity profiles are modulated in the overlap region as a consequence of interference. The radiance distribution pre-

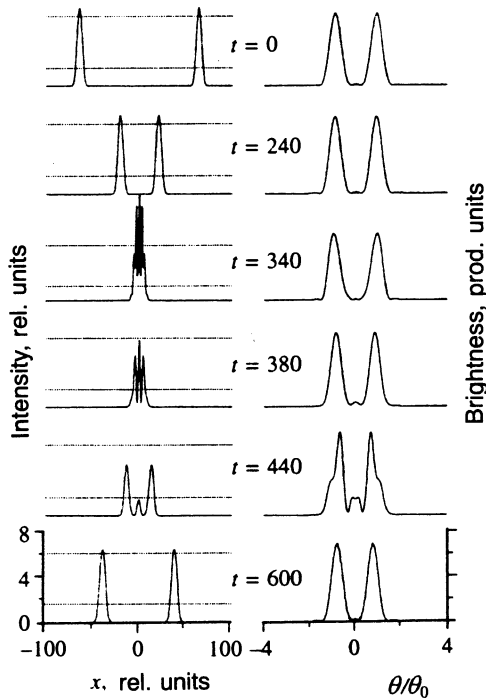


FIG. 7. Intensity profiles (left) and radiance distribution (right) for the weak interaction regime ($\theta_{1,2} = \pm 0.16\theta_0$).

serves the form of two symmetric, separated peaks with width $\sim \theta_d = \lambda/w_0$ and maxima at the angles $\theta_{1,2} = v_{1,2}/c$. The result of the collision remains the same, in fact in a wider region than described by inequality (4.7) (see Fig. 7): A new factor here is the appearance during the overlap time of an additional peak in the angular distribution (radiance), and also in the spatial profile (Fig. 7, $t=380$ and 440). This is caused by interference of the fields of the colliding autosolitons. Regions of depressed total intensity arise in the laser, where the local saturated gain exceeds the losses. The resulting amplification is preserved for the paraxial rays ($\theta \approx 0$), for which rays the tails of the initial angular distributions serve as initiators. Therefore, during the collision time the central peak grows until it reaches some finite value. This value is small if the collision time is short ($\sim w_0/\delta v$). After the collision this central peak dissipates (Fig. 7, $t=600$).

For a corresponding decrease in the initial velocity the central peak grows during the collision time to some critical value. Above this critical value, the peak stabilizes after the collision and is converted into an additional laser autosoliton (Fig. 8, $t > 400$). This (central) soliton is stationary, and the finite velocities of the receding laser autosolitons are somewhat less than the original velocities (under the conditions of Fig. 8, 1.5 times less). The modulation frequency of the angular distribution of the receding and, correspondingly, non-interacting solitons (Fig. 8, $t=980$) increases; the reason for this was explained at the beginning of this section.

If the velocities of the two initial laser autosolitons are still less, then their angular distributions strongly overlap and are strongly modulated (Fig. 9, $t=0$). As they approach, the central peak in the angular distribution, corresponding to $\theta=0$, grows and dominates. As a result, the two initial soli-

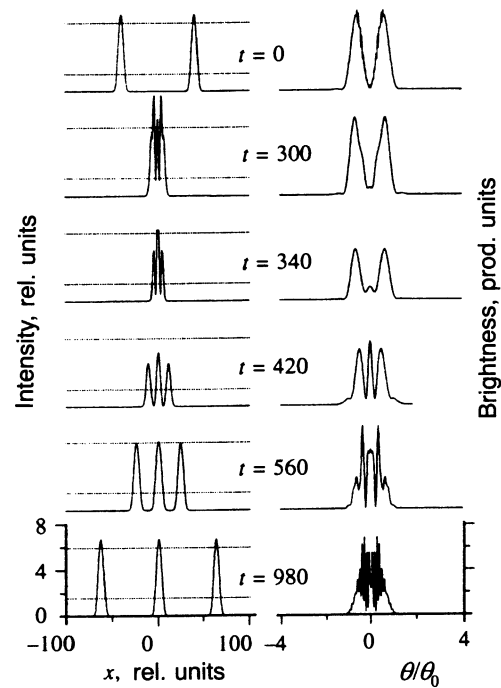


FIG. 8. Formation of a third autosoliton in a collision of two autosolitons ($\theta_{1,2} = \pm 0.10\theta_0$).

tons coalesce into one immobile soliton (Fig. 9, $t=900$).

At very small velocities, the dynamics of the collision of the laser autosolitons again changes. The interaction of the solitons at first reduces their relative motion. They approach to some minimum distance (Fig. 10, $t=1000$), after which they move apart with decreased velocity (approximately two times less). Thus, slowly moving laser autosolitons repel.

These results suggest that there are difference between laser autosolitons and diffraction autosolitons in a nonlinear interferometer, for which relatively small velocities of transverse motion are characteristic, but for which interaction leads to the formation of bound structures ("polyatomic mol-

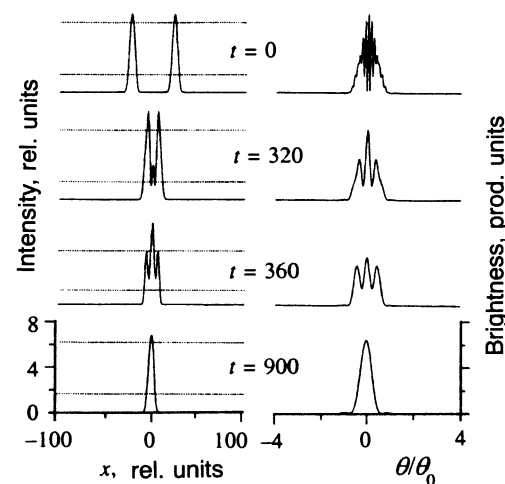


FIG. 9. Coalescence of two autosolitons ($\theta_{1,2} = \pm 0.048\theta_0$).

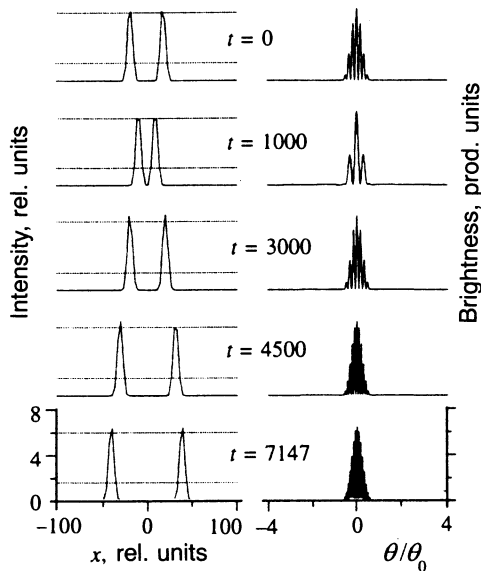


FIG. 10. Repulsion of laser autosolitons ($\theta_{1,2} = \pm 0.008\theta_0$).

ecules" with a discrete set of distances between the individual "atoms"). These differences are due to the different asymptotic behavior of the field at the periphery of the individual solitons: with increasing distance from the center the intensity falls off monotonically for laser autosolitons, and with oscillations for diffraction autosolitons. Depending on the distance between neighboring autosolitons, the presence of oscillations causes their regions of attraction and repulsion to alternate, leading to a discrete spectrum of equilibrium distances between the diffraction autosolitons.^{7,9}

In general, two initial laser autosolitons can differ in their speeds ($|v_1| \neq |v_2|$) and phases ($\Phi_2 \neq \Phi_1$). The first of these two factors is not of any fundamental significance since with the help of transformation (2.6) we can always transform to a system associated with the motion of the "center of inertia," in which $v_2 = -v_1$. At the same time, the result of the collision depends substantially on the phase difference of the initial laser autosolitons, especially for values of the parameters corresponding to the boundaries between the different collision regimes. To illustrate, it is sufficient to compare Figs. 11a and b, for which the only difference in the initial conditions is the phase differences. Whereas Fig. 11a demonstrates the passage of one laser autosoliton through another, Fig. 11b demonstrates the formation of an additional soliton moving with transverse velocity equal to the arithmetic mean of the velocities of the initial solitons.

5. CONCLUSION

Our analysis of laser autosolitons leads us to the following conclusions:

There exist stable laser autosolitons not only with regular wavefront, but also with screw dislocations of the wavefront of different orders.

A laser autosoliton moving in the transverse direction toward the edge of a mirror disappears if the angle of incidence exceeds a critical value. It is reflected from the edge,

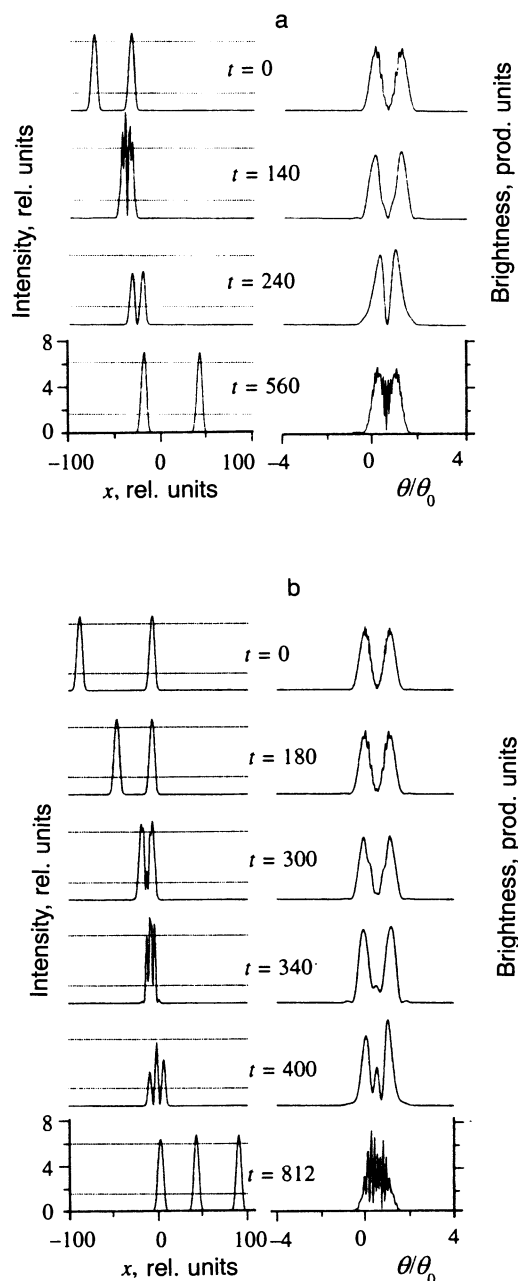


FIG. 11. Change in the regime with variation of the phase difference of the autosolitons ($\theta_1 = 0.2\theta_0$, $\theta_2 = 0$).

thereby converting into an autosoliton with its corresponding velocity component opposite in sign and somewhat decreased in absolute value if the angle of incidence is less than critical. The critical angle is close to the diffraction width of a single autosoliton.

The result of the collision of two initially separated laser autosolitons is determined, for given laser parameters, by the initial values of their relative velocity and phase difference. As the relative velocity decreases, the following regimes occur successively: 1) the autosolitons pass through one another with restoration of their original velocities after the collision; 2) as a result of the collision, in addition to the two receding autosolitons, an additional autosoliton localized be-

tween them develops, moving with velocity equal to the arithmetic mean of the velocities of the original autosolitons; 3) the two autosolitons coalesce into one with velocity equal to the arithmetic mean of the velocities of the two original autosolitons; 4) the initial autosolitons approach to some minimum distance with subsequent repulsion, then separate with relative velocity somewhat less in magnitude than the magnitude of the initial relative velocity.

This work was carried out with partial support of the International Scientific Fund (Project R53000).

- ¹V. I. Bepalov and V. I. Talanov, *Pis'ma Zh. Eksp. Teor. Fiz.* **3**, 471 (1966) [*JETP Lett.* **3**, 307 (1966)].
- ²A. A. Mak, L. N. Soms, V. A. Fromzel', and V. E. Yashin, *Neodymium-Glass Lasers* [in Russian], Nauka, Moscow (1990).
- ³Y. Silberberg, *Opt. Lett.* **15**, 1282 (1990).
- ⁴N. N. Rozanov and V. E. Semënov, *Opt. Spektrosk.* **48**, 108 (1980) [*Opt. Spectrosc.* **48**, 59 (1980)].
- ⁵B. S. Kerner and V. V. Osipov, *Autosolitons* [in Russian], Nauka, Moscow (1991).
- ⁶N. N. Rozanov and G. V. Khodova, *Opt. Spektrosk.* **65**, 1375 (1988) [*Opt. Spectrosc.* **65**, 810 (1988)].
- ⁷N. N. Rosanov and G. V. Khodova, *J. Opt. Soc. Am. B* **7**, 1057 (1990).
- ⁸A. N. Rakhmanov, *Opt. Spektrosk.* **74**, 1184 (1993) [*Opt. Spectrosc.* **74**, 701 (1993)].
- ⁹N. N. Rosanov, *Proc. SPIE*, Vol. 1840, 130 (1992).
- ¹⁰Yu. I. Balkarei, A. V. Grigor'yants, Yu. A. Rzhano, and M. I. Elinson, *Opt. Commun.* **66**, 161 (1988).
- ¹¹N. N. Rozanov, S. V. Fëdorov, *Opt. Spektrosk.* **72**, 1394 (1992) [*Opt. Spectrosc.* **72**, 782 (1992)].
- ¹²S. V. Fëdorov, G. V. Khodova, and N. N. Rozanov, *Proc. SPIE*, Vol. 1840, 208 (1992).
- ¹³V. N. Lisitsyn and V. P. Chebotaev, *Zh. Eksp. Teor. Fiz.* **54**, 419 (1968) [*Sov. Phys. JETP* **27**, 227 (1968)].
- ¹⁴N. N. Rozanov, *Opt. Spektrosk.* **77**, No. 3, (1994). [*Opt. Spectrosc.* **77**, (1994)].
- ¹⁵V. A. Malomed, *Physica D* **29**, 155 (1987).
- ¹⁶K. A. Gorshkov and L. A. Ostrovsky, *Physica D* **3**, 428 (1981).
- ¹⁷N. N. Rozanov, *Opt. Spektrosk.* **76**, 621 (1994) [*Opt. Spectrosc.* **76**, (1994)].
- ¹⁸A. F. Suchkov, *Zh. Eksp. Teor. Fiz.* **49**, 1495 (1965) [*Sov. Phys. JETP* **22**, 1026 (1966)].
- ¹⁹L. F. Lugiato and R. Lefever, *Phys. Rev. Lett.* **21**, 2209 (1967).
- ²⁰N. N. Rosanov, A. V. Fëdorov, S. V. Fëdorov, and G. V. Khodova, *Proc. SPIE*, Vol. 2039, 330 (1993).
- ²¹N. N. Rozanov, *Opt. Spektrosk.* **52**, 548 (1982) [*Opt. Spectrosc.* **52**, 326 (1982)].
- ²²L. A. Vaïnshteïn, *Diffraction and the Factorization Method* [in Russian], Soviet Radio, Moscow (1964).
- ²³Yu. A. Anan'ev, *Optical Resonators and Laser Beams* [in Russian], Nauka, Moscow (1990).
- ²⁴I. S. Aranson, K. A. Gorshkov, A. S. Lomov, and M. I. Rabinovich, *Physica D* **43**, 435 (1990).
- ²⁵N. N. Rosanov, in *Progress in Optics*, ed. by E. Wolf, North-Holland, Amsterdam (1995), in press.

Translated by Paul F. Schippnick